Press, Tucson, 1979), pp. 926–924; C. Y. Shih *et al.*, *Geochim. Cosmochim. Acta* **46**, 2323 (1982); G. Dreibus *et al.*, *Lunar Planet. Sci.* **XIII**, 186 (1982); N. Nakamura, H. Komi, H. Kagami, *Meteoritics* **17**, 257 (1982); H. Y. McSween, *ibid.* **29**, 757 (1994).
4. D. D. Bogard and P. Johnson, *Science* **221**, 651 (1983).
5. R. H. Becker and R. O. Pepin, *Earth Planet. Sci. Lett.* **69**, 225 (1984).
6. A. O. Nier and M. B. McElroy, *J. Geophys. Res.* **82**, 4341 (1977); T. Owen and K. Biemann, *Science* **193**, 801 (1976); T. Owen *et al.*, *J. Geophys. Res.* **82**, 4635 (1977).
7. Noble gas signatures in whole-rock samples of shergottites show only slight excesses of ^{40}Ar and ^{129}Xe (*16, 20, 21*), and a shock-melt glass from LEW 88516 revealed excesses of ^{40}Ar and ^{129}Xe, with no associated heavy N (*22*).
8. L. L. Watson, I. D. Hutcheon, S. Epstein, E. M. Stolper, *Science* **265**, 86 (1994).
9. T. Owen, J. P. Maillard, C. de Bergh, B. L. Lutz, *ibid.* **240**, 1767 (1988).
10. T. J. McCoy, G. J. Taylor, K. Keil, *Geochim. Cosmochim. Acta* **56**, 3571 (1992).
11. E. Stolper and H. Y. McSween, *ibid.* **43**, 1475 (1979).
12. M. Wadhwa, T. J. McCoy, K. Keil, G. Crozaz, *Meteoritics* **28**, 453 (1993).
13. H. Y. McSween and E. Jarosewich, *Geochim. Cosmochim. Acta* **47**, 1501 (1983).
14. D. Stoeffler *et al.*, *ibid.* **50**, 889 (1986).
15. $\delta^{15}N$ (per mil) = 1000 $\{[(^{15}N/^{14}N)_{sample}/(^{15}N/^{14}N)_{Earth\ atm}]-1\}$.
16. D. D. Bogard, L. E. Nyquist, P. Johnson, *Geochim. Cosmochim. Acta* **48**, 1723 (1984).
17. O. Eugster, *Meteoritics* **29**, 464 (1994).
18. J. S. Kim, Y. Kim, K. Marti, *Lunar Planet Sci.* **XXV**, 701 (1994); in preparation.
19. R. C. Wiens, R. H. Becker, R. O. Pepin, *Earth Planet. Sci. Lett.* **77**, 149 (1986).
20. T. D. Swindle, M. W. Caffee, C. M. Hohenberg, *Geochim. Cosmochim. Acta* **50**, 1001 (1986).
21. U. Ott, *ibid.* **52**, 1937 (1988).
22. R. H. Becker and R. O. Pepin, *Meteoritics* **28**, 637 (1993).
23. D. D. Bogard, F. Hörz, P. H. Johnson, *J. Geophys. Res.* **91**, E99 (1986).
24. R. C. Wiens and R. O. Pepin, *Geochim. Cosmochim. Acta* **52**, 295 (1988).
25. J. S. Kim *et al.*, in preparation.
26. S. Epstein and H. P. Taylor, *Geochim. Cosmochim. Acta Suppl.* **2**, 1421 (1971).
27. J. S. Kim and K. Marti, *Lunar Planet Sci.* **XXII**, 145 (1992).
28. K. Biemann, T. Owen, D. R. Rushneck, A. L. LaFleur, D. W. Howarth, *Science* **194**, 76 (1976).
29. E. Anders and N. Grevasse, *Geochim. Cosmochim. Acta* **53**, 197 (1989).
30. We thank G. J. MacPherson and R. Haag for providing samples of Zagami for this work, T. Graf for discussions, and two anonymous reviewers for constructive suggestions. We thank T. Servilla, T. Tatnall, and T. Hulsebosch for technical assistance. Supported by National Aeronautics and Space Administration grants NAGW-3428 to K.M., and NAGW-3281 to K.K. A.N.T. was supported by the California Space Grant Consortium at the University of California at San Diego. Hawaii Institute of Geophysics and Planetology publication 795 and School of Ocean and Earth Science and Technology publication 3821.

21 October 1994; accepted 9 January 1995

Crystal Structure of the β Chain of a T Cell Antigen Receptor

Graham A. Bentley,* Ginette Boulot, Klaus Karjalainen, Roy A. Mariuzza*

The crystal structure of the extracellular portion of the β chain of a murine T cell antigen receptor (TCR), determined at a resolution of 1.7 angstroms, shows structural homology to immunoglobulins. The structure of the first and second hypervariable loops suggested that, in general, they adopt more restricted sets of conformations in TCR β chains than those found in immunoglobulins; the third hypervariable loop had certain structural characteristics in common with those of immunoglobulin heavy chain variable domains. The variable and constant domains were in close contact, presumably restricting the flexibility of the β chain. This may facilitate signal transduction from the TCR to the associated CD3 molecules in the TCR-CD3 complex.

Antigen recognition by T lymphocytes is mediated by highly diverse cell-surface glycoproteins known as T cell receptors. These disulfide-linked heterodimers are composed of α and β (or γ and δ) chains consisting of variable (V) and constant (C) regions homologous to those of antibodies (*1, 2*). Although antibodies generally recognize antigens in their native form, αβ TCRs recognize antigens as peptides bound to molecules of the major histocompatibility complex (MHC) (*3*). In addition, TCRs interact with a class of molecules known as superantigens, which stimulate T cells bearing particular V_β elements (*4*). We now report the crystal structure at 1.7 Å resolution of the extracellular portion of the β chain ($V_\beta 8.2 J_\beta 2.1 C_\beta 1$) of a TCR (designated 14.3.d) specific for a hemagglutinin peptide of influenza virus [HA(110–120)] presented by the MHC class II I-E^d molecule (*5*). Production (*6*), crystallization (*7*), and structure determination (*8*) of the recombinant β chain are described below.

The TCR β chain is divided into V and C domains structurally homologous to the V and C domains of immunoglobulins (Fig. 1, A and B). The root-mean-square (rms) difference in α carbon positions is 1.4 Å with respect to V_L (compared with framework residues from nine murine V_L domains) and 1.9 Å with respect to V_H (compared with framework residues from nine murine V_H domains). The framework structure of V_β is therefore closer to that of V_L. For C_β, the structural difference with immunoglobulin homologs is greater. Sequence alignment by structural homology (Table 1) gives rms differences between 2.3 and 3.0 Å for the α carbon positions of matched residues. The C_β domain contains a large, solvent-exposed insertion with respect to other immunoglobulin C domains between residues 219 to 232 (inclusive) (Fig. 1). Sequence comparisons suggest that this insertion also occurs in C_γ domains from mice and humans. Thus, the number of amino acids between the last intrachain disulfide bridge and the interchain bridge is 34 for mouse C_β, 32 for human C_γ form 1 (*9*), 31 for mouse $C_\gamma 1$, and 26 for $C_\gamma 2$; for the immunoglobulin C_κ and $C_H 1$ domains, these are 18 and 19 residues long, respectively (*10*).

Peptide loops homologous to the complementarity-determining regions (CDRs) of immunoglobulins are disposed on the V domain to form part of the expected antigen-binding site (Figs. 1 and 2). A significant difference with respect to immunoglobulins, however, occurs in CDR1 of $V_\beta 8.2$. In both V_L and V_H domains, CDR1 is largely stabilized by the hydrophobic side chain of residue 29, which is positioned midway along this loop and oriented to intercalate between two β-pleated sheets in a nonpolar environment. By contrast, His^{29} of $V_\beta 8.2$ is displaced sideways relative to the immunoglobulin homolog and is partially exposed to the solvent (Fig. 3A). The volume occupied by residue 29 in immunoglobulin V domains is instead taken by Gln^{25} in $V_\beta 8.2$. In this configuration, the amide group of Gln^{25} stabilizes CDR1 by forming four hydrogen bonds to its main chain atoms. The CDR1 sequences of many V_β domains are similar to that of $V_\beta 8.2$ by virtue of their common length and the presence of Gln and a hydrophilic residue at positions 25 and 29, respectively. Thus, sequences listed by Kabat *et al.* (*10*) for the murine subgroup II of V_β have the same number of residues in CDR1 in which Gln^{25} and His^{29} are invariant residues. Similarly, in subgroup I Gln^{25} occurs 11 times and His^{29} occurs 35 times in 37 sequences, and all but one CDR1 have the same length. The structure described here for $V_\beta 8.2$ may therefore be common to many other V_β CDR1 structures.

Structural alignment of the $V_\beta 8.2$ domain with immunoglobulin V domains shows that the β chain CDR2 is equal in

G. A. Bentley and G. Boulot, Unite d'Immunologie Structurale (CNRS URA 359), Institut Pasteur, 25 rue du Dr Roux, 75724 Paris Cedex 15, France.
K. Karjalainen, Basel Institute for Immunology, Grenzacherstrasse 487, Postfach CH-4005, Basel, Switzerland.
R. A. Mariuzza, Center for Advanced Research in Biotechnology, University of Maryland, 9600 Gudelsky Drive, Rockville, MD 20850, USA.

*To whom correspondence should be addressed.

Table 1. Alignment of the C_β sequence with immunoglobulin constant domain sequences (C_H1, C_H2, C_H3, and C_κ) based on structural information. The α carbon skeletons were first optimally superimposed. Sequences were then manually adjusted to minimize the number of gaps while respecting the structural similarity. The rms differences in α carbon positions between the 89 matched residues of C_β and C_H1, C_H2, C_H3, and C_κ are 3.0 Å, 2.3 Å, 2.3 Å, and 2.7 Å, respectively. Conserved amino acids are indicated by vertical bars. The insertion of C_β residues 219 to 232 relative to immunoglobulin constant domains is underlined. Single-letter abbreviations for the amino acid residues are as follows: A, Ala; C, Cys; D, Asp; E, Glu; F, Phe; G, Gly; H, His; I, Ile; K, Lys; L, Leu; M, Met; N, Asn; P, Pro; Q, Gln; R, Arg; S, Ser; T, Thr; V, Val; W, Trp; and Y, Tyr.

Domains	Sequence
C_β	EDLRQVTPPKVSLFEPSKAE-IANKQKATLVCLARGFF--PDHVELSWWVNGKEV-HSGVSTDPQAY
C_H1	ASTTPPSVFPLAPGSA--AQTNSMVTLGCLVKGYF--PEPVTVTWN--SGSL-SSGVHTFP-AV
C_H2	PSVFLFPPKPKDTLMISRTPEVTCVVVDVSHEDPQVKFNWYVDGVQVHNAKTKPR--EQ
C_H3	PREPQVYTLPPSRE--EMTKNQVSLTCLVKGFY--PSDIAVEWESNGQPE--NNYKTTP-PV
C_κ	RADAAPTVSIFPPSSE--QLTSGGASVVCFLNNFY--PKDINVKWKIDGSER-QNGVLDS--WT
C_β	KES--NYSHCLSSRLRVSATFWHNPRNHFRCQVQFHGLSEEDKWPEGSPKPVTQNISAEAWG
C_H1	LQS---DLYTLSSSVTVPSSPRPS--ETVTCNVAHPA----------SSTKVDKKIVPRD
C_H2	QYN---STYRVVSVLTVLHQNWLDG-KEYKCKVSNKA----------LPAPIEKTISK
C_H3	LDS--DGSFFLYSKLTVDKSRWQQG-NVFSCSVMHEAL----------HNHYTQKSLSL
C_κ	DQDSKDSTYSMSSTLTLTKDEYERH-NSYTCEATHKT----------STSPIVKSFNRN

length to the H chain CDR2 of the solved Fab structures NEW, HyHEL-10, D1.3, and AN02 (*11*, *12*). Although these V_H domains each form a three-residue loop within CDR2, that of V_β8.2 is seven residues long because each β strand forming the hairpin loop is reduced by two residues by comparison with that of V_H. The seven-residue loop is stabilized by the side chain of Ser^{49}, which forms hydrogen bonds to the main chain atoms (Fig. 3B). The Arg^{69} residue may also have an important influence on the conformation of CDR2; the guanidyl group forms a hydrogen bond to Oγ of Ser^{49} and its carbonyl oxygen forms a hydrogen bond to the main chain at residue 53. Because CDR2 of subgroup II V_β is constant in length, and Ser^{49} and Arg^{69} are invariant, the conformation observed here may be common to these β chains.

The restricted conformational heterogeneity of CDR1 and CDR2 of the β chain suggested by the above analysis is compatible with models of peptide-MHC recognition in which these CDRs are thought to contact primarily the α-helical regions of the MHC molecule (*2*, *13*), which also display rather limited structural diversity (*14*). However, the close juxtaposition of both CDR1 and CDR2 to CDR3 (which is believed to interact mainly with bound peptide) in the putative peptide-MHC binding site probably precludes an exclusive assignment of particular functions to individual CDRs.

Figure 2 shows the location of the β chain CDRs relative to the so-called fourth hypervariable region (HV4), which has been implicated in superantigen binding (*4*). This region, comprising residues 69 to 75 (*15*), forms a loop that folds toward CDR1 and CDR2 like the homologous region of V_L domains. In V_H domains, by contrast, this loop is almost always directed away toward the solvent. The continuous surface formed by the CDRs and HV4 in the crystal structure (Fig. 2) could explain the existence of mutational and genetic evidence that certain residues in CDR1 and CDR2 of the β chain may modulate binding to superantigens (*16*–*18*). Other residues implicated in superantigen recognition, including V_β8.2 Asn^{24} (*19*), are also in close proximity to HV4 in our model. The possibility that HV4 of TCR V domains may be implicated in peptide-MHC recognition has already been raised (*20*). Because it folds toward CDR1 and CDR2 in the crystal structure, it is indeed more favorably placed to contact the MHC-peptide complex than if it were V_H-like in conformation. Furthermore, the idiotope–anti-idiotope complex, FabD1.3-FabE225, offers an example where antibody-antigen contacts are mediated by the third framework region (FR3) residues of V_L (*21*), which are equivalent by homology to residues of HV4 in V_β.

The hydrophobic surface of the V_β domain that, by analogy to immunoglobulins, should form the interface with V_α in the αβ heterodimer does indeed contact the same surface of a neighboring β chain in the crystal lattice. Instead of forming an immunoglobulin Fv-like structure, however, the two V domains pack head-to-tail such that their CDR loops appear on opposite sides of the dimeric aggregate. Several residues at this interface, however, are equivalent by homology to those involved in the V_H-V_L interaction. Dimerization of V_β domains to an Fv-like configuration is prevented, at least in part, by the conformation of CDR3. As observed with V_H domains, this loop

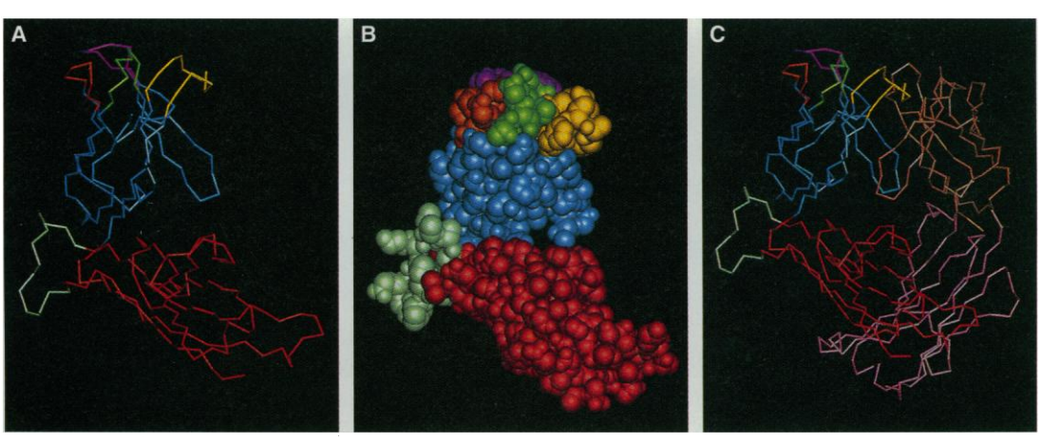

Fig. 1. The β chain (V_β8.2J_β2.1C_β1). (**A**) An α carbon skeleton of the β chain with V_β (blue), C_β (red), CDR1 (green), CDR2 (violet), CDR3 (yellow), HV4 (orange), and the insertion residues, 219 to 232, of C_β (gray). (**B**) A space-filling model viewed from the same orientation and with the same color code as in (A). (**C**) A model for the αβ TCR heterodimer based on the β chain [colored as in (A)] and V_L (brown) and C_L (pink) immunoglobulin chains viewed from the same orientation as in (A).

folds away from the core of the domain, and thus away from CDR1 and CDR2 (Fig. 2), so that steric encumbrance between adjacent CDR3 loops of such a homodimer would indeed prevent its formation. To permit αβ dimerization, the CDR3 loop of the α chain would have to fold back over the surface of the V_α domain toward CDR1 and CDR2, as found with V_L domains. Consistent with this prediction, a recombinant TCR V_α domain has been found to form stable homodimers in solution (*22*), in a manner reminiscent of that of L chain dimers (Bence-Jones proteins) (*23*).

By contrast with that of V_β, the surface of the C_β domain implicated in heterodimer formation is completely exposed to solvent. This surface has a constellation of charged residues (carrying a net positive charge) that cannot be neutralized by a complementary matching of the same surface of a neighboring C_β domain. This contrasts with immunoglobulin C domains, where the dimer-forming surface is very hydrophobic and carries no charged residues except at the periphery. We note in addition that the predicted dimer-forming surface of the C_α domain is also rather polar and should carry a net negative charge (*1*). Polar residues may therefore be disposed such that charges are neutralized by salt-bridge formation across the C_α-C_β interface in the heterodimer. Similar considerations should apply to the interaction between pre-TCRα (*24*) and C_β in the pre-TCR complex.

The V_β and C_β domains are in intimate contact in the crystal structure (Fig. 1). In all, 18 residues together with three bridging solvent molecules contribute toward contacts between the surfaces of the two domains. Although this total includes those residues [Val^{12}, Thr^{115}, Val^{116A} (*10*), Phe^{153}, and Pro^{154}] predicted by extrapolation from immunoglobulin H chain structures (*2*, *25*), these do not appear to make the most important contacts in the case of the β chain. Rather, these are made by J_β residues Arg^{113} and Thr^{115} and C_β residues Glu^{158} and His^{156}. Thus, Arg^{113} is involved in numerous nonpolar interactions across the V_β-C_β interface and forms a salt bridge to Glu^{158} that could help maintain the β chain in a restricted quaternary configuration. Several van der Waals contacts are also established between His^{156} and residues from the V domain, including a hydrogen bond between Nε2 and Oγ of Thr^{115}. It is noteworthy that murine J_β genes code for Arg [present in five out of six sequences (*10*)] or for Lys at position 113 and that residue 115 is also relatively conserved, with Thr (four sequences), Ser, or Leu appearing at this position. A similar situation arises in human J_β sequences (*10*). These additional and more significant interactions are correlated with a larger surface of interaction between the V_β and C_β domains than is found in immunoglobulin H chains. The combined surface area between the two domains that is inaccessible by solvent is 833 $Å^2$ (the contribution of residues 116A and 117 at the transition between the two domains was not included). Corresponding areas between immunoglobulin V_H and C_H1 domains vary between about 200 $Å^2$ and 350 $Å^2$, depending on the elbow angle.

In the absence of the α chain, an important question posed by the crystal structure concerns whether the arrangement of the V_β and C_β domains described above is compatible with an Fab-like quaternary structure for an αβ heterodimer. To examine this possibility, we superimposed the V_H domain of a V_H-V_L dimer onto the V_β domain and the C_H1 domain of a C_H1-C_L dimer onto the C_β domain to determine if the resulting positions of the V_L and C_L domains would be disposed to form a plausible model for the α chain in an αβ heterodimer. The superposition placed V_L and C_L in a configuration consistent with a contiguous polypeptide for the α chain in which steric encumbrance between the two domains was negligible (Fig. 1C). The model of the complete αβ heterodimer thus obtained closely resembled an Fab fragment with an elbow angle of about 154°, well within the bounds of those angles observed for immunoglobulin structures.

For several reasons, we believe the close association between V_β and C_β found in the crystal structure may represent a biologically relevant conformation of the β chain and is not a result of the absence of an α chain or its particular packing in the crystal lattice. First, the relatively compact structure is consistent with the resistance of the β chain to a variety of proteases, whether or not it is paired with an α chain (*26*). Second, nearly all the contacts between the V_β and C_β domains are mediated by V region residues that are highly conserved across different V_β families. Third, modeling studies indicate that an immunoglobulin L chain may be paired with the β chain without altering the latter's conformation. Fourth, the close association of V_β and C_β domains is consistent with the results of V-C shuffling experiments, which suggest that αβ TCR V and C domains are not structurally autonomous units (*27*), in contrast to antibody V and C domains (*28*).

Should the quaternary arrangement of the β chain reported here be preserved in the αβ heterodimer, we would anticipate a rigid structure largely devoid of flexibility in the region homologous to the elbow of an Fab fragment, given the extensive interaction between the V_β and C_β domains. This, in turn, may have important implications for signal transduction, because a rigid conformation could facilitate the transmission of any structural changes, which may occur in the TCR upon binding the peptide-MHC complex, to associated CD3 molecules in the TCR-CD3 complex (*29*). In

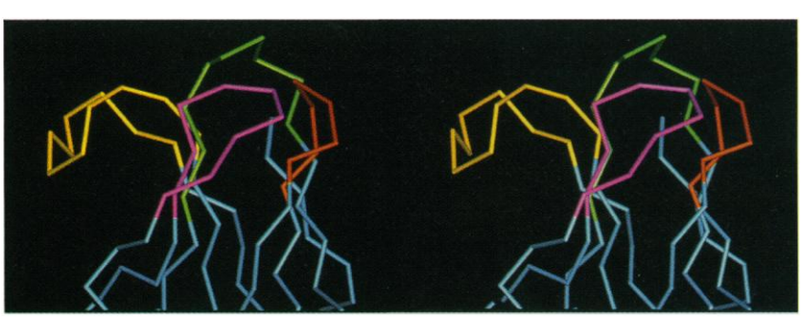

Fig. 2. A stereo view of the α carbon skeleton of V_β showing the framework regions (blue), CDR1 (green), CDR2 (pink), CDR3 (yellow), and HV4 (orange).

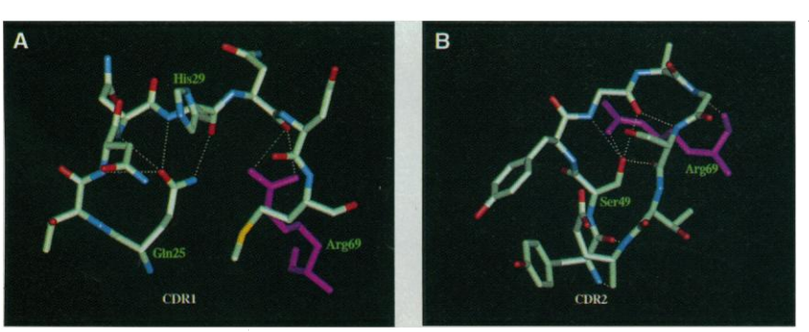

Fig. 3. Hypervariable regions of the β chain. (**A**) CDR1, residues 25 to 33. (**B**) CDR2, residues 48 to 56. Residue Arg^{69}, which interacts with CDR1 and CDR2, is shown in violet.

the case of antibodies, by contrast, the structural independence of V and C domains (*28*), together with the much larger separation expected between the V domains and putative signal-transducing molecules on the cell surface (*30*), effectively rules out an allosteric mechanism to account for B cell activation. In this respect, the large protruding loop on the external face of the C_β domain (and possibly of the C_γ domain), comprising residues 219 to 232 (Fig. 1), could be particularly important in contacting the extracellular portions of CD3 molecules, thereby helping to couple the antigen recognition and signal transduction functions of the TCR-CD3 complex.

REFERENCES AND NOTES

1. Y. Yanagi *et al.*, *Nature* **308**, 145 (1984); S. M. Hedrick, E. A. Nielsen, J. Kavaler, D. I. Cohen, M. M. Davis, *ibid.*, p. 153; J. Novotny, S. Tonegawa, H. Saito, D. R. Kranz, H. N. Eisen, *Proc. Natl. Acad. Sci. U.S.A.* **83**, 742 (1986).
2. C. Chothia, D. R. Boswell, A. M. Lesk, *EMBO J.* **7**, 3745 (1988).
3. J. B. Rothbard and M. L. Gefter, *Annu. Rev. Immunol.* **9**, 527 (1991).
4. B. L. Kotzin, D. Y. M. Leung, J. Kappler, P. Marrack, *Adv. Immunol.* **54**, 99 (1993).
5. S. Weber, A. Traunecker, F. Oliveri, W. Gerhard, K. Karjalainen, *Nature* **356**, 793 (1992).
6. We initially obtained crystals of a glycosylated form of the 14.3.d β chain (*26*). As these diffracted only to medium resolution, however, site-directed mutagenesis was used to eliminate four out of the five potential NH_2-linked glycosylation sites. Asparagines at positions 24, 74, and 121 were mutated to glutamine, and Ser^{283}, which is COOH-terminal to Asn^{236}, was mutated to valine. The prototype vector containing immunoglobulin locus elements (*31*) was used to drive expression of the mutated complementary DNA corresponding to the rearranged V_β and the first C region exon of the TCR β gene. Soluble β chain was produced in myeloma cells and purified from culture supernatants (~10 mg/ml) by a single affinity chromatography step with the C_β monoclonal antibody H57-597 (*32*). The unmutated NH_2-linked glycosylation site at position 186 was used only in a few of the chains (<10%), as judged by SDS–polyacrylamide gel electrophoresis. A homogeneous product was obtained by treatment of the native protein with neuraminidase and glycosidases.
7. Protein solution [5.8 mg/ml in 7.3 mM tris, 25 mM Hepes (pH 7.5), 18.3 mM NaCl, 1.0% (w/v) polyethylene glycol (PEG) 4000, 0.75% (saturated) ammonium sulfate, and 0.014% agarose] was used to form a sitting drop, which was equilibrated by vapor diffusion over a buffer reservoir of higher concentration (4% PEG 4000, 0.1 M Hepes, and 3% ammonium sulfate at pH 7.25). Crystals (0.4 mm by 0.4 mm by 0.1 mm) usually grew within a period of about 3 weeks. They belong to the space group *C*2 with unit cell parameters a = 100.6 Å, b = 36.6 Å, c = 71.5 Å, and β = 113.4°.
8. A data set was collected with a MARresearch (Hamburg, Germany) imaging plate system mounted on the wiggler line DW32 at the synchrotron at LURE (Laboratory for the Utilization of Electromagnetic Radiation), Orsay, France. A total of 60,827 reflections were obtained from a single crystal to yield a set of 25,371 unique observations (R_{sym} = 0.049), which was 95.6% complete at a resolution between 15.0 and 1.7 Å. (For the outer resolution shell, 1.76-1.70 Å, R_{sym} was 0.399 with 95.1% completeness and 34% having $I > 3\sigma$.) A preliminary model for the β chain was obtained by molecular replacement with the program AMoRe (*33*) with V_L from HyHEL-10 (*12*) and C_H1 as search models. The structure was refined with the program X-PLOR (*34*) during the preliminary stages, then with the CCP4 (*35*) version of PROLSQ (*36*) for the final steps. The *R* factor of the refined model is 0.198 for 21,745 reflections, with $F > 3\sigma$ in the resolution range of 7.0 to 1.7 Å (0.208 for all 23,577 reflections in this resolution range). The rms deviations of bonds and angles from the target values are 0.013 Å and 2.0°, respectively. The final model of the β chain included all 238 residues in the main chain trace of the recombinant molecule and 107 solvent molecules.
9. F. Hochstenbach and M. B. Brenner, *J. Clin. Immunol.* **10**, 1 (1990).
10. E. A. Kabat, T. T. Wu, H. M. Perry, K. S. Gottesman, C. Foeller, *Sequences of Proteins of Immunological Interest* (Public Health Services, National Institutes of Health, Washington, DC, ed. 5, 1991).
11. NEW: F. Saul and R. J. Poljak, *Struct. Funct. Genet.* **14**, 363 (1992); D1.3: T. O. Fischmann *et al.*, *J. Biol. Chem.* **266**, 12915 (1991); AN02: A. T. Brünger, D. J. Leahy, T. R. Hynes, R. O. Fox, *J. Mol. Biol.* **211**, 239 (1991).
12. HyHEL-10: E. A. Padlan *et al.*, *Proc. Natl. Acad. Sci. U.S.A.* **86**, 5938 (1989).
13. M. M. Davis and P. J. Bjorkman, *Nature* **334**, 395 (1988); J.-M. Claverie, A. Prochnicka-Chalufour, L. Bougueleret, *Immunol. Today* **10**, 10 (1989).
14. D. H. Fremont, M. Matsumura, E. A. Stura, P. Peterson, I. A. Wilson, *Science* **257**, 919 (1992); J. H. Brown *et al.*, *Nature* **364**, 33 (1993).
15. R. Jores, P. M. Alzari, T. Meo, *Proc. Natl. Acad. Sci. U.S.A.* **87**, 9138 (1990).
16. P. A. Patten *et al.*, *J. Immunol.* **150**, 2281 (1993).
17. J. Kang, C. A. Chambers, J. Pawling, C. Scott, N. Hozumi, *ibid.* **152**, 5305 (1994).
18. P. A. Cazenave *et al.*, *Cell* **63**, 717 (1990).
19. A. M. Pullen, T. Wade, P. Kappler, J. W. Kappler, *ibid.* **61**, 1365 (1990).
20. P. Patten *et al.*, *Nature* **312**, 40 (1984).
21. G. A. Bentley, G. Boulot, M. M. Riottot, R. J. Poljak, *ibid.* **348**, 254 (1990).
22. B. A. Fields *et al.*, *J. Mol. Biol.* **239**, 339 (1994).
23. M. Schiffer, R. L. Girling, K. R. Ely, A. B. Edmundson, *Biochemistry* **12**, 4620 (1973).
24. C. Saint-Ruf *et al.*, *Science* **266**, 1208 (1994).
25. A. M. Lesk and C. Chothia, *Nature* **335**, 188 (1988).
26. G. Boulot, G. A. Bentley, K. Karjalainen, R. A. Mariuzza, *J. Mol. Biol.* **235**, 795 (1994).
27. G. Casorati, A. Traunecker, K. Karjalainen, *Eur. J. Immunol.* **23**, 586 (1993).
28. T. Simon and K. Rajewsky, *EMBO J.* **9**, 1056 (1990).
29. K. Karjalainen, *Curr. Opin. Immunol.* **6**, 9 (1994).
30. M. Reth, *Annu. Rev. Immunol.* **10**, 97 (1992).
31. A. Traunecker, F. Oliveri, K. Karjalainen, *Trends Biochem. Sci.* **9**, 109 (1991).
32. R. T. Kubo, W. Born, J. W. Kappler, P. Marrack, M. Pigeon, *J. Immunol.* **142**, 2736 (1989).
33. J. Navaza, *Acta Crystallogr.* **A50**, 157 (1994).
34. A. T. Brünger, *X-PLOR Version 3.1: A System for X-ray Crystallography and NMR* (Yale Univ. Press, New Haven, 1992).
35. Collaborative Computing Project Number 4, *Acta Cryst.* **D50**, 760 (1994).
36. W. A. Hendrickson, *Methods Enzymol.* **115**, 252 (1985).

37. We thank J. Montreuil, University of Lille, for aid in characterizing the carbohydrate of the β chain. Supported by grants from the Institut Pasteur and CNRS. The Basel Institute for Immunology was founded and is supported by F. Hoffmann–La-Roche, Switzerland.

12 December 1994; accepted 23 February 1995

Regional Forest Fragmentation and the Nesting Success of Migratory Birds

Scott K. Robinson,* Frank R. Thompson III, Therese M. Donovan, Donald R. Whitehead, John Faaborg

Forest fragmentation, the disruption in the continuity of forest habitat, is hypothesized to be a major cause of population decline for some species of forest birds because fragmentation reduces nesting (reproductive) success. Nest predation and parasitism by cowbirds increased with forest fragmentation in nine midwestern (United States) landscapes that varied from 6 to 95 percent forest cover within a 10-kilometer radius of the study areas. Observed reproductive rates were low enough for some species in the most fragmented landscapes to suggest that their populations are sinks that depend for perpetuation on immigration from reproductive source populations in landscapes with more extensive forest cover. Conservation strategies should consider preservation and restoration of large, unfragmented "core" areas in each region.

The conservation of neotropical migrant bird species, which breed in North America and winter in the tropics, has attracted attention even though most are not yet endangered (*1*, *2*). Many neotropical migrants, however, are suffering population declines, the causes for which may include the loss of breeding, wintering, and migration stopover habitats (*3*). A frequently hypothesized cause for declines in populations of migrant birds is the negative impact of habitat fragmentation (*4*) on breeding success (*5*). Habitat fragmentation may allow higher rates of brood parasitism by brown-headed cowbirds (*Molothrus ater*) and nest predation (*6*, *7*). Cowbirds lay their eggs in the nests of other "host" species, which then raise cowbirds at the expense of their own young (*8*).

Populations of cowbirds and many nest predators are higher in fragmented landscapes where there is a mixture of feeding habitats (agricultural and suburban) and breeding habitats (forests and grasslands) (*8*–*10*). In landscapes fragmented by agri-

S. K. Robinson, Illinois Natural History Survey, 607 East Peabody Drive, Champaign, IL 61820, USA.
F. R. Thompson III, North Central Forest Experiment Station, University of Missouri, Columbia, MO 65211, USA.
T. M. Donovan and J. Faaborg, Division of Biological Sciences, University of Missouri, Columbia, MO 65211, USA.
D. R. Whitehead, Department of Biology, Indiana University, Bloomington, IN 47405, USA.
*To whom correspondence should be addressed.